Braz J Phys (2012) 42:6–13
DOI 10.1007/s13538-011-0054-x

SBF SOCIEDADE BRASILEIRA DE FÍSICA

CONDENSED MATTER

Vibrational Spectroscopic Investigation on Some M(Benzonitrile)$_2$Ni(CN)$_4$ Complexes (M = Ni, Zn, Cd, and Hg)

Zeki Kartal

Received: 1 February 2011 / Published online: 4 January 2012

Abstract The first synthesis of benzonitrile tetracyanonickelate complexes, represented by the general formula M(benzonitrile)$_2$Ni(CN)$_4$ (M = Ni, Zn, Cd, and Hg), is reported. Fourier transform infrared spectroscopy and Raman spectroscopic data in the region of 4,000–400 cm^{-1} are presented, and the vibrational frequencies are assigned and explained in detail. The thermal behavior of these complexes was also investigated by thermogravimetric analysis, differential thermal analysis, and derivative thermal gravimetric analysis. The spectral and thermal analysis results of the newly synthesized complexes suggest that these complexes are new examples of Hofmann-type complexes. The spectral data obtained show that the complexes consist of $|M–Ni(CN)_4|_\infty$ polymeric layers with the ligand (benzonitrile) molecules bound to metal through the N-donor atom of the cyanide group.

Keywords Tetracyanonickelate · IR spectroscopy · Raman spectroscopy · Thermal analysis · Hofmann-type complexes · Benzonitrile · Square planar polymeric layers

1 Introduction

In 1897, the young German chemist Karl A. Hofmann (1870–1940) chanced to obtain the complex Ni(CN)$_2$·NH$_3$·C$_6$H$_6$, a discovery that ultimately led to a new class of clathrates. The clathrates are complexes in which a molecule of one substance, the guest, is caged in a host lattice of another one; the word clathrate stems from the Greek radical clathri, meaning lattice. The structure of the first Hofmann-type clathrate was determined by Powell and Rayner in 1949–1952 [1, 2], and then Hofmann's formula was revised to [Ni(NH$_3$)$_2$Ni(CN)$_4$]·2C$_6$H$_6$.

In the following decade, much study was dedicated to the potential use of clathrates to separate hydrocarbon components of petroleum distillates. More recently, numerous applications exploited the caging properties of the complexes, which have been employed as catalysts and anti-oxidants, as stabilizing agents in chemistry, pharmacology, and several industries, such as the fabrication of cosmetics, and as molecular sieves for chemical purification and isomer separation [3–10]. The Hofmann-type clathrates are of the form [MLM′(CN)$_4$]·2G, the host being called a Hofmann-type complex. In Hofmann's prototypical compound, the host is a diamminemetal(II) tetracyanometallate(II) metal complex, the ligand L being NH$_3$, and both transition metals M and M′ being Ni. The guest G is C$_6$H$_6$.

A variety of other Hofmann-type complexes has been produced, with different ligands. As one would expect, the properties of the host structure depends both on the ligand molecule and the transition metal atoms [10]. The transition metal M is one of the elements Mn, Fe, Co, Ni, Cu, Zn, or Cd, with valence +2, in an octahedral environment. M′ is also divalent; it can either belong to the sequence Ni, Pd, Pt and be surrounded by a square-planar environment, or to the sequence Zn, Cd, Hg, surrounded by a tetrahedral environment. The ligand L is either one bidentate molecule or two monodentate molecules, which donate electrons

Z. Kartal (✉)
Department of Physics, Dumlupınar University,
43100 Kütahya, Turkey
e-mail: zkartal@dumlupinar.edu.tr

to the partially filled d (or f) shells of the transition metals; depending on the ligand and the metal, the resulting covalent bond can range from very weak to very strong, considerable polar character being often observed [11]. The Hofmann-type complexes comprise two-dimensional polymeric layers $MLM'(CN)_4$, formed by $[ML]^{2+}$ cations and $[M'(CN)_4]^{2-}$ ($M' = Ni$, Pd, or Pt) anions. Depending on the shape and size of the ligand, different structural cavities are formed between the polymeric layers, in which the guest molecule is imprisoned [3–9, 12]. Since the complexes are prepared in aqueous environments, water molecules can invade the cavities, as can water molecules from moisture in the air.

In this study, we report the synthesis of four new candidates to Hofmann-type complexes with the benzonitrile (BN) molecule as ligand. We also report Fourier transform infrared spectroscopy (FT-IR) measurements of the spectra in the 4,000–400 cm^{-1} range, in which we identify vibrational frequencies that are expected in Hofmann-type complex structures. In addition, we report thermogravimetric analysis (TGA), differential thermogravimetric analysis (DTGA), and differential thermal analysis (DTA) curves in the temperature range 20–700°C, which indicate that, upon heating, water molecules leave the compounds, followed by the benzonitrile molecules and that, at higher temperatures, the cyanide molecules are decomposed. Combined with the vibrational spectra, the thermal analyses confirm that we have obtained Hofmann-type complexes with benzonitrile ligands, the first ones to our knowledge.

2 Experimental

2.1 Materials and Syntheses of the Complexes

All the chemicals, namely BN (C_6H_5CN; Fluka, 99%), $NiCl_2 \cdot 6H_2O$ (Fluka, 98%), $ZnCl_2 \cdot 6H_2O$ (Fluka, 99%), $CdCl_2 \cdot 2H_2O$ (Fluka, 96%), $HgCl_2$ (Merck, 98%), and $K_2[Ni(CN)_4] \cdot aq$ (Fluka, 98%), were used without further purification. The complexes were prepared by the following method: First, 1 mmol of $K_2[Ni(CN)_4] \cdot aq$ was dissolved in distilled water, and 2 mmol of BN was added to the solution under stirring. Then 1 mmol of MCl_2 (M = Ni, Zn, Cd, and Hg), dissolved in distilled water, was added to this mixture. The whole mixture was stirred for around a week at room temperature. The obtained complexes were filtered; washed with pure water, ethanol, and ether; and dried in desiccators containing silica gel.

2.2 Instrumentation

The FT-IR spectra of these complexes in powder form were recorded at room temperature with a Bruker VERTEX 70 FT-IR spectrometer between 4,000 and 400 cm^{-1} with a resolution of 2 cm^{-1} using a Harrick MVP2 single reflection ATR accessory with a diamond crystal. The Raman spectra of these complexes in powder form were recorded in the region of 4,000–400 cm^{-1} with Bruker Senterra dispersive Raman microscope using the 532-nm line of a 3B diode laser. The TGA and DTA curves of the these complexes were recorded under air at a heating rate of 10°C/min in the temperature area 20–700°C using platinum crucibles on a SII EXSTAR 6000 TG/DTA 6300 thermal analyzer.

The freshly prepared complexes were analyzed for metals amounts with Perkin-Elmer optima 4300 DV ICP-OES and for C, H, and N amounts with CHNS-932 (LECO) elemental analyzer. The results of elemental analysis, given in Table 1, indicate that there is approximately half a molecule of water in a unit cell of the complexes. This can also be seen in the results of the thermal analysis.

3 Results and Discussion

The FT-IR and Raman spectra of $M(BN)_2Ni(CN)_4$ (M = Ni, Zn, Cd, and Hg) complexes are compatible

Table 1 Elemental analysis of the M–BN–Ni (M = Ni, Zn, Cd, and Hg) complexes

Abbreviations of complexes and M_r (g)	Elemental analysis, found (%)/(calculated) (%)						
	H	C	N	Ni	Zn	Cd	Hg
$Ni(C_6H_5CN)_2Ni(CN)_4.(0.5)H_2O$ (Ni–BN–Ni) $M_r = 436.71$	2.62 (2.54)	48.79 (49.51)	18.71 (19.24)	26.19 (26.88)	–	–	–
$Zn(C_6H_5CN)_2Ni(CN)_4.(0.5)H_2O$ (Zn–BN–Ni) $M_r = 443.40$	2.73 (2.50)	48.43 (48.76)	18.59 (18.95)	12.73 (13.24)	14.58 (14.75)	–	–
$Cd(C_6H_5CN)_2Ni(CN)_4.(0.5)H_2O$ (Cd–BN–Ni) $M_r = 490.43$	2.49 (2.26)	43.47 (44.08)	17.01 (17.14)	11.49 (11.97)	–	22.34 (22.90)	–
$Hg(C_6H_5CN)_2Ni(CN)_4.(0.5)H_2O$ (Hg–BN–Ni) $M_r = 578.61$	1.69 (1.92)	37.24 (37.37)	14.12 (14.52)	10.31 (10.14)	–	–	33.76 (34.67)

with each other and are shown in Fig. 1. The spectra show that the complexes have analogous spectral features. The vibrational results obtained from the spectral data can be analyzed for the vibration of the BN ligand and the $[Ni(CN)_4]^{2-}$ ions individually to follow the possible shifts taking place in the complexion, which are explained below starting with the ligand molecule vibrations.

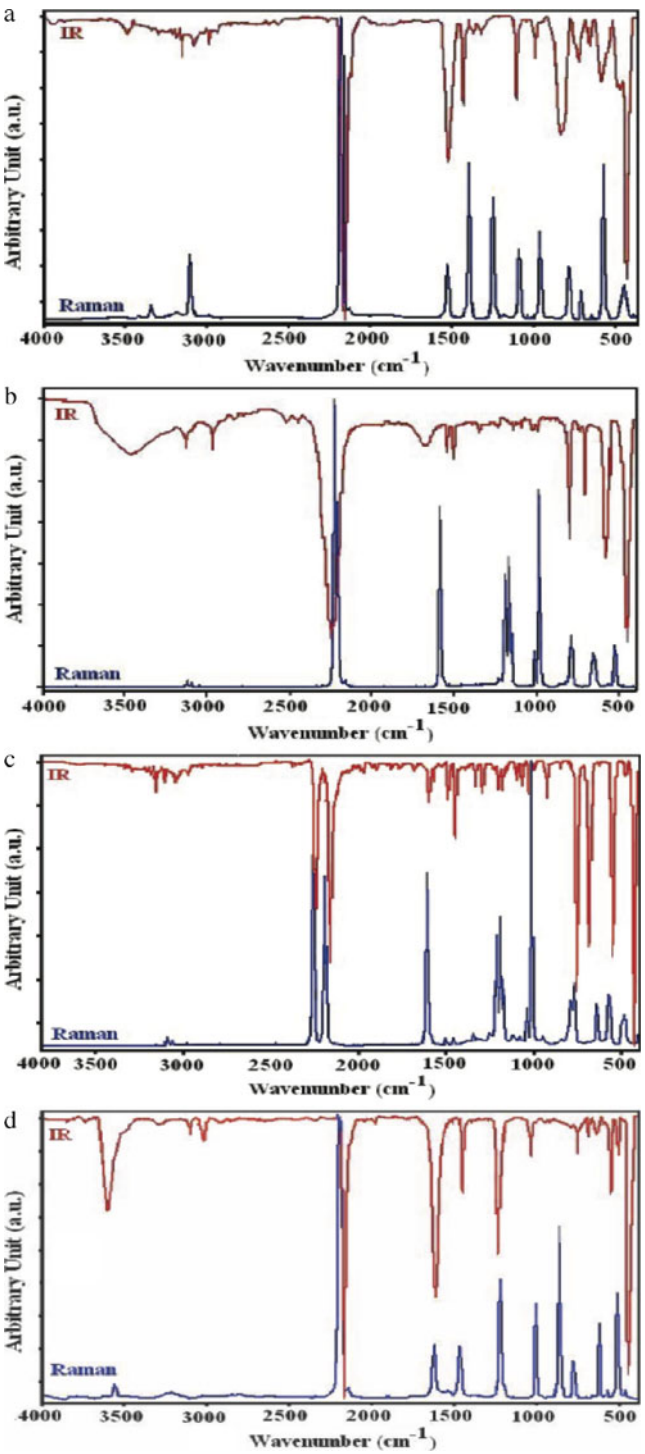

Fig. 1 The IR and Raman spectra of the Ni–BN–Ni (**a**), Zn–BN–Ni (**b**), Cd–BN–Ni (**c**), and Hg–BN–Ni (**d**) complexes

3.1 Benzonitrile Vibrations

A nitrile is any organic compound which has a $-C\equiv N$ (cyanide) functional group. The cyanide group includes also an electronegative nitrogen atom. The BN molecule has a very interesting character in that three different binding sites (aromatic ring, π-bond of CN group, and lone pair electrons of nitrogen atom) are available for interaction with the transition metal atoms. The BN can form coordination complexes with late transition metals that are both soluble in organic solvents. The BN ligands are readily displaced by stronger ligands, making BN complexes useful synthetic intermediates. The BN is used as a solvent and chemical intermediate for the synthesis of pharmaceutical, dyestuffs, and rubber chemicals through the reactions of alkylation, condensation, hydrolysis, halogenations, or nitration. BN and its derivatives are used in the manufacture of lacquers, polymers, and anhydrous metallic salts as well as intermediates for pharmaceutical, agrochemicals, and other organic chemicals. The molecular structure of BN is shown in Fig. 2.

The electron densities of the BN were calculated at the restricted Hartree–Fock level using PM3 method in MOPAC 97 program packet. It has been seen that the nitrogen atom has a higher electron density than all the other atoms. According to this, we expect that the BN molecule bonds to transition metals via nitrogen atom in our complexes. In the literature, several studies were made with the BN molecule [13–23]. In the present study, the vibrational band assignments of the BN molecule are based on the results by Dimitrova [22].

The BN molecule has a planar structure and belongs to the C_{2v} symmetry. It has 33 normal modes of vibration, namely $\Gamma = 12A_1 + 3A_2 + 7B_1 + 11B_2$. Four

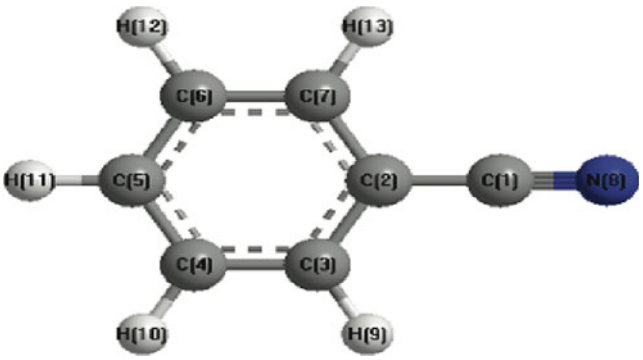

Fig. 2 The molecular structure of the BN

of these are Raman active, 18 are IR active, and 11 are both IR and Raman active [16, 21, 22]. The BN molecule is a monodentate ligand. The assignments and wavenumbers of the vibrational bands of the BN molecule in the spectra of the $M(BN)_2Ni(CN)_4$ complexes are listed in Table 2, together with the wavenumbers of the BN in liquid phase.

In the FT-IR and Raman spectrums of the studied complexes, the observed small frequency shifts are due to the changes of the environment of the BN molecule and also due to the pairing of the internal vibration of the BN molecule with the vibrations of the M–N band, without connecting the BN molecule to the complex. However, significant shifts are observed in the stretching frequency of the CH and cyanide group.

The frequencies of the [νCH (4,6,3,7) (A_1)] and [νCH (4,6,3,7) (B_2)] in the infrared spectrum of the liquid BN molecules at 3,081 and 3,030 cm^{-1} shifted to a low-frequency region around 4–8 and 25–50 cm^{-1} in complexes, respectively. The frequencies of the [νCH (4,6,3,7) (A_1)] and [νCH (4,6,3,7) (B_2)] in the Raman spectrum of the liquid BN molecules at 3,083 and 2,984 cm^{-1} and the [νCH (4,6,3,7) (A_1)] shifted to a low-frequency region around 5–22 cm^{-1} and the [νCH (4,6,3,7) (B_2)] shifted to a high-frequency region around 13–40 cm^{-1} in complexes, respectively.

The CN stretching vibration frequency observed at the 2,230 cm^{-1} with 10 cm^{-1} bandwidth in the infrared spectrum of the liquid BN molecule is shifted to a lower-frequency region around 33–51 cm^{-1} with 22–24 cm^{-1} bandwidth in the Zn–BN–Ni and Ni–BN–Ni complexes. However, the same frequency is shifted to a higher-frequency region around 17–34 cm^{-1} with 23–26 cm^{-1} bandwidth in the Cd–BN–Ni complex and Hg–BN–Ni complex, respectively. The CN stretching vibration frequency observed at the 2,241 cm^{-1} in the Raman spectrum with 9 cm^{-1} bandwidth of the liquid BN molecule is shifted to a lower-frequency region around 14–53 cm^{-1} with 20–24 cm^{-1} bandwidth in the Ni–BN–Ni, Zn–BN–Ni, and Hg–BN–Ni complexes. The same frequency is shifted to a higher-frequency region around 18 cm^{-1} with 19 cm^{-1} bandwidth in the

Table 2 The vibrational absorption wavenumbers (per centimeter) of liquid BN and M–BN–Ni complexes (M = Ni, Zn, Cd, and Hg)

	Assignment[a]	Liquid BN		Ni–BN–Ni		Zn–BN–Ni		Cd–BN–Ni		Hg–BN–Ni	
		IR	Raman	IR	Raman	IR	Raman	IR	Raman	IR	Raman
1	νCH (3,7,4,6) (B_2)	3,087 sh	–	–	–	–	–	–	–	–	–
2	νCH (4,6,3,7) (A_1)	3,081 m	3,083 m	3,077 w	3,065vw	3,073 w	3,077 vw	3,076 w	3,061 vw	3,073 w	3,078 w
3	νCH (4,6,3,7) (B_2)	3,030 w	2,984 vw	2,998 vw	2,997 vw	2,980 w	3,023 vw	2,999 w	3,010 vw	3,005 w	–
4	νCN (1) (A_1)	2,230 vs	2,241 vs	2,179 s	2,188 vs	2,197 s	2,227 vs	2,247 s	2,259 vs	2,264 s	2,189 vs
5	νCC (9,12) (A_1)	1,602 s	1,615 m	1,595 m	1,615 w	1,599 w	1,610 s	1,596 m	1,615 s	1,600 m	1,608 m
6	νCC (10,11,8,13) (B_2)	1,587 m	–	1,583 w	–	1,580 w	–	1,584 w	–	1,585 vw	–
7	CH def.(17,19,16,20) (A_1)	1,497 s	1,503 vw	1,490 vw	–	1,489 m	1,502 m	1,488 m	1,501 vw	1,489 w	1,508 vw
8	CH def. (18,17,19) (B_2), νCC (9,12) (B_2)	1,450 s	1,461 vw	1,448 vw	1,457 vw	1,447 m	1,456 vw	1,447 m	1,458 vw	1,448 m	1,454 w
9	CH def. (16,20) (B_2)	1,333 m	–	1,339 vw	–	1,334 vw	–	1,332 w	–	1,335 w	–
10	νCC (8,13,9,12) (B_2)	1,288	–	1,288 w	–	1,287 w	–	1,290 w	–	1,290 w	–
11	CH def (17,19)(A_1), νCC (9,12) (A_1), νCC′(2)(A_1)	–	1,198 m	–	1,208 vw	–	1,210 w	–	1,216 m	–	1,214 w
12	CH def (16,20) (A_1)	1,179 s	–	1,165 w	–	1,178 w	–	1,178 w	–	1,177 w	–
13	νCC (9,12), CH def. (16,20) (B_2)	1,072 s	1,083 w	1,068 w	1,078 w	1,071 w	1,079 vw	1,068 w	1,080 vw	1,068 w	1,079 w
14	νCC (10,11) (A_1)	1,029 s	1,040 w	1,025 s	1,039vw	1,024 w	–	1,025 s	1,038 w	1,026 w	1,037 vw
15	Ring def (21) (A_1)	1,002 m	1,014 s	1,000 w	1,013 w	999 w	1,013 s	998 w	1,014 s	999 w	1,014 m
16	CH wag (26,30,28) (B_1)	922 s	–	926 w	–	927 w	–	924 m	–	925 w	–
17	CH wag(27,29,26,30)(A_2)	845 m	845 w	–	856 w	851 vw	854	848 vw	841 vw	860 w	854 m
18	Ring def (31) (B_1)	756 vs	773 w	756 w	773 w	762 s	777 w	756 s	770 m	754 s	775 m
19	Ring def (31) (B_1)	688 vs	–	685 vw	–	688 m	–	683 s	–	683 s	–
20	Ring def (31) (B_2)	615 w	638 w	626 vw	646 w	631 vw	638 vw	627 vw	640 w	628 vw	638 vw
21	CCN linear bend(24)(B_1)	542 vs	562 w	567 m	567 m	576 s	565 w	552 s	569 w	569 m	573 m
22	νCC′ (2)(A_1), Ring def (22) (A_1)	462 w	475 w	obsc.	491 w	461 vw	473 vw	472 w	483 w	470 vw	480 vw

ν stretching, δ deformation, *s* strong, *m* medium, *w* weak, *v* very, *sh* shoulder, *obsc.* obscured by $Ni(CN)_4$ band
[a]From [22]

Cd–BN–Ni complex. As a result, substantial change of frequencies and band broadening occurred implying the direct bonding of the cyanide group with the transition metal atoms [24]. Similar higher-frequency shifts are also observed for the other different ligands having cyanide group in the structure [14–16].

From the previous studies of the metal–nitrile complexes and the nitriles absorbed on the metal surface using various techniques, it has commonly been accepted that the linear coordination (σ-bonding) through the nitrogen lone pair electrons results in an increase in the ν(CN) frequency from the free molecule. On the other hand, coordination through the C≡N π system is known to result in a decrease in the ν(CN) frequency from the free molecule [16, 20, 24]. It is seen that a linear relation exists between amounts of high-frequency shift and the place of transition metal in the periodic table. That is, the shift to a high frequency in complexes depends on the masses and the electronegativity of transition metals. All of these results reflect the direct interaction of the CN group with the M transition metal atoms (M = Ni, Zn, Cd, and Hg) [14, 20]. In addition, the CCN linear bending frequency shows a shift to a high-frequency region around 4–28 cm^{-1} wavenumbers in complexes. This shift results from binding of the ligand molecules to the transition metal atoms. As the strength of CN–M band increases, the CCN linear-bend out-of-plane vibration frequencies increase as well.

Small frequency shifts appear due to coupling between interior vibrations of ligand with M–N bonding vibrations, for example [νCC (9,12) (A_1)]; [CH def (17,19,16,20)(A_1)]; [CH def(17,19) (A_1), νCC (9,12) (A_1), νCC′ (2) (A_1)]; [Ring def (31) (B_1)]; [Ring def (31) (B_2)], and [νCC′ (2) (A_1), Ring def (22) (A_1)]. The [νCC (9,12) (A_1)] stretching vibration frequency observed at the 1,602 cm^{-1} in the infrared spectrum of the liquid BN molecule is shifted to a lower-frequency region around 2–7 cm^{-1} in the all complexes. The [νCC (9,12) (A_1)] stretching vibration frequency observed at the 1,615 cm^{-1} in the Raman spectrum of the liquid BN molecule is shifted to a lower-frequency region around 5–7 cm^{-1} in the all complexes. The [CH def (17,19,16,20) A_1)] vibration frequency observed at the 1,497 cm^{-1} in the infrared spectrum of the liquid BN molecule is shifted to a lower-frequency region around 7–9 cm^{-1} in the all complexes. The [CH def (17,19,16,20)(A_1)] vibration frequency observed at the 1,503 cm^{-1} in the Raman spectrum of the liquid BN molecule is shifted to a lower-frequency region around 1–2 cm^{-1} in Ni–BN–Ni, Zn–BN–Ni, and Cd–BN–Ni complexes. The same frequency is shifted to a higher-frequency region around 5 cm^{-1} in the Hg–BN–Ni complex. The [CH def (17,19) (A_1),νCC (9,12) (A_1), νCC′ (2) (A_1)] vibration frequency observed at the 1,198 cm^{-1} in the Raman spectrum of the liquid BN molecule is shifted to a higher-frequency region around 10–17 cm^{-1} in the all complexes. The [Ring def (31) (B_1)] vibration frequency observed at the 688 cm^{-1} in the infrared spectrum of the liquid BN molecule is shifted to a lower-frequency region around 3–5 cm^{-1} in the all complexes. The [Ring def (31) (B_2)] vibration frequency observed at the 615 cm^{-1} in the infrared spectrum of the liquid BN molecule is shifted to a higher-frequency region around 11–16 cm^{-1} in the all complexes. The [Ring def (31) (B_2)] vibration frequency observed at the 638 cm^{-1} in the Raman spectrum of the liquid BN molecule is shifted to a higher-frequency region around 0–8 cm^{-1} in the all complexes.

The [νCC′ (2) (A_1), Ring def (22) (A_1)] vibration frequency observed at the 462 cm^{-1} in the infrared spectrum of the liquid BN molecule is shifted to a higher-frequency region around 8–10 cm^{-1} in the all complexes. The [νCC′(2) (A_1), Ring def (22) (A_1)] vibration frequency observed at the 475 cm^{-1} in the Raman spectrum of the liquid BN molecule is shifted to a higher-frequency region around 5–16 cm^{-1} in Ni–BN–Ni, Cd–BN–Ni, and Hg–BN–Ni, complexes. The same frequency is shifted to a lower frequency region around 2 cm^{-1} in the Zn–BN–Ni complex. It is obvious that the observed FT-IR peaks between 3,613 and 3,100 cm^{-1} result from the small amount water molecules in the $M(BN)_2Ni(CN)_4$ (M = Ni, Zn, Cd, and Hg) complexes [14].

3.2 $[Ni(CN)_4]^{2-}$ Vibrations

The structure of the unit cell of $[Ni(CN)_4]^{2-}$ ions is shown in Fig. 3. If a unit cell has the symmetry D_{4h}, then nine normal modes are expected to be in a vibration spectrum. Four of them must be active in the IR spectrum and the remaining in the Raman spectrum.

Fig. 3 Unit cell of $[Ni(CN)_4]^{2-}$ ions

The IR active vibrational modes are E_u δ(CN), E_u ν(Ni–CN), A_{2u} π(Ni–CN), and E_u δ(Ni–CN). Since we have observed these four bands in the infrared spectrum, our complexes have a square planar environment. The frequencies of the $Ni(CN)_4$ group vibrations in complexes are assigned on the basis of the work of McCullough et al. [25], who presented vibrational data for the ion $Ni(CN)_4$ in $Na_2Ni(CN)_4$. The vibrational wave numbers of the $Ni(CN)_4$ in our complexes are given in Table 3, together with the data for the complexes of Ni–CPN–Ni [26] for comparison.

As the stretched vibrations of the ν_8(CN), E_u of the $K_2Ni(CN)_4$ in the infrared spectrum were observed in 2,122 cm^{-1} region, the band ν_8(CN), E_u for the complex of M–BN–Ni was shifted to the high-frequency range around 40–65 cm^{-1}. As the stretched vibrations of the ν_1(CN), A_{1g} and ν_4(CN), B_{1g} of the $K_2Ni(CN)_4$ in the Raman spectrum were observed in 2,149 and 2,141 cm^{-1} region, respectively, the band ν_1(CN), A_{1g} for the all complex of M–BN–Ni was shifted to the high-frequency range around 27–62 cm^{-1}. The band ν_4(CN), B_{1g} is shifted to a lower-frequency region around 6–7 cm^{-1} in the Ni–BN–Ni and Cd–BN–Ni complexes, and the same frequency is shifted to a higher-frequency region around 3–22 cm^{-1} in the Zn–BN–Ni and Hg–BN–Ni complexes, respectively. Furthermore, the value of the CN stretching vibration frequencies depends on other factors, such as electronegativity of metal, coordination number, and oxidation state [27, 28].

The same shift occurred also in the in-plane bending δ(Ni–CN), E_u for the complexes around 12–20 cm^{-1}. The shifts show that both bands are connected to the transition metal atoms. These shifts affiliated with metal result from coupling of the CN stretching vibrations and metal–nitrogen bond stretching vibrations. The ν_9(Ni–CN), E_u were observed as a medium intensity band at 567 cm^{-1} for Ni–(BN)–Ni, at 549 cm^{-1} for Zn–(BN)–Ni and Hg–(BN)–Ni, and at 552 cm^{-1} for Cd–(BN)–Ni complex.

The characteristic ν(CN) and δ(Ni–CN) frequencies observed are similar to the Hofmann-type complexes indicating that the $|M–Ni(CN)_4|_\infty$ layers were preserved [29]. Therefore, $[Ni(CN)_4]^{2-}$ anions and $[M–(BN)_2]^{2+}$ cations come together in square planar sheet constitution. These polymeric layers are held in parallel by Van der Waals interactions between BN molecules. The α-type cavity occurs in these complexes. The cavities have volume depending on the type of transition metals. The BN molecules are located below and above the plane. Nickel atoms are surrounded by four carbon atoms of cyanide groups and M metal atoms are also surrounded by four nitrogen atoms of the cyanide groups, and at the same time, two nitrogen atoms of nitrile group of the BN molecules are bonded to the metal atoms in the regular square plane.

4 Thermal Behavior of Complexes

The TGA, DTA, and DTG graphics of all the complexes are compatible, and Ni–BN–Ni, Zn–BN–Ni, Cd–BN–Ni, and Hg–BN–Ni complexes are shown in Fig. 4. The TGA results indicate that samples are stable at room temperature. By heating, however, all of complexes gradually lose their water and ligand molecules between about 60°C and 171°C. The water molecules in the cavities of complexes and bounded weakly to the complexes leave in the first decomposition stage low-temperature range 60–71°C [found (calc.) % = 2.14 (2.06) for Ni–BN–Ni, 2.10 (2.03) for Zn–BN–Ni, % = 1.73 (1.84) for Cd–BN–Ni, and 1.68 (1.56) for Hg–BN–Ni].

The second and third decomposition stages around 88–103°C and 121–172°C indicate that the BN molecules leaves from the M–BN–Ni (M = Ni, Zn, Cd, and Hg) complexes [found (calc.) % = 47.07 (47.23) for Ni–BN–Ni, 46.30 (46.51) for Zn–BN–Ni, % = 41.73 (42.05) for Cd–BN–Ni, and 35.46 (35.64) for Hg–BN–Ni]. The final decomposition stage around 379–436°C

Table 3 Vibrational wavenumbers $Ni(CN)_4$ group in M–BN–Ni complexes (per centimeter)

Assignment[a]	$Na_2Ni(CN)_4$[a]	Ni–CPN–Ni[b]	Ni–BN–Ni	Zn–BN–Ni	Cd–BN–Ni	Hg–BN–Ni
ν_1(CN), A_{1g}	(2,149)	–	(2,184) vs	(2,211) s	(2,179) vs	(2,176) s
ν_4(CN), B_{1g}	(2,141)	–	(2,135) vs	(2,163) w	(2,134) s	(2,144) w
ν_8(CN), E_u	2,132 vs	2,174 vs	2,179 s	2,187 s	2,162 s	2,179 s
ν_9(Ni–CN),E_u	543 w	570 m	567 m	549 m	552 m	549 m
δ(Ni–CN), E_u	433 s	438 w	453 s	452 s	430 s	445 s

The bands in the Raman spectra appear within parentheses
vs very strong, *s* strong, *m* medium, *w* weak
[a]From [25]
[b]From [26]

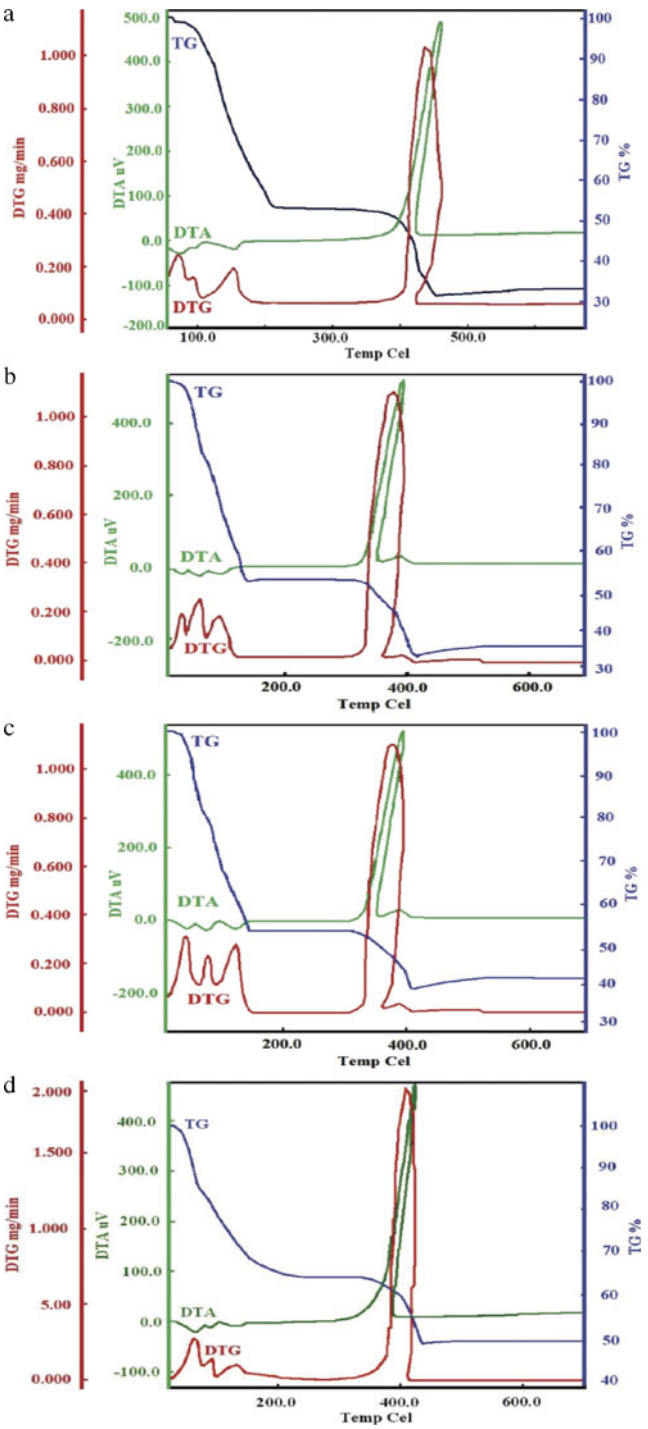

Fig. 4 The TGA, DTA, and DTG curves are of the Ni–BN–Ni (**a**), Zn–BN–Ni (**b**), Cd–BN–Ni (**c**) and Hg–BN–Ni (**d**) complexes

is the decomposition of cyanide to yield the respective metal oxide [found (calc.) % = 34.14 (34.21) for Ni–BN–Ni, 35.10 (35.20) for Zn–BN–Ni, % = 41.53 (41.41) for Cd–BN–Ni, and 50.26 (50.34) for Hg–BN–Ni]. The results show the formation of the complex. The decomposition temperatures of M–BN–Ni (M = Ni, Zn, Cd, or Hg) complexes are given in Table 4. Similar decomposition stages have been observed for other Hofmann-type complexes [30, 31] and Hofmann-type clathrates [32–35].

Table 4 Decomposition temperatures of the M–BN–Ni complexes (M = Ni, Zn, Cd, or Hg)

Sample	Decomposition (°C)			
	I	II	III	IV
Ni–BN–Ni	70.9	94.0	154.3	436.4
Zn–BN–Ni	60.3	96.4	120.6	379.1
Cd–BN–Ni	61.4	102.9	171.6	427.6
Hg–BN–Ni	61.8	87.7	131.2	407.4

5 Conclusions

The BN molecules acts as a monodentate ligand and bonds to transition metal atoms through nitrogen atom of CN group in the four new complexes prepared M–BN–Ni (M = Ni, Zn, Cd, and Hg) successfully. The FT-IR and Raman spectroscopic studies of four new Hofmann-type complexes have shown that they have similar structures consisting of infinite two-dimensional polymeric layers formed with $[Ni(CN)_4]^{2-}$ ions bridged by $[M(BN)_2]^{2+}$ (M = Ni, Zn, Cd, and Hg) cations. These polymeric layers are held in parallel by Van der Walls interactions between the BN molecules. The complexes $M(Benzonitrile)_2Ni(CN)_4$ (M = Ni, Zn, Cd, and Hg) are new examples of Hofmann-type complexes.

Acknowledgements The author wishes to thank in particular Anadolu University for providing technical assistance and Dumlupınar University for the technical and financial support with the project number 46. The author is also indebted to Prof. Dr. Mustafa ŞENYEL for the use of the Bruker Senterra Dispersive Raman Microscope.

References

1. H.M. Powell, J.H. Rayner, Nature **163**, 566 (1949)
2. J.H. Rayner, H.M. Powell, J. Chem. Soc. **319** (1952)
3. M. Hagan, *Clathrate Inclusion Compounds* (Chapman & Hall, London, 1962), p. 189
4. J.L. Atwood, J.E. Davies, T. Osa, *Clathrate Compounds, Molecular Inclusion Phenomena and Cyclodextrins (Advances in Inclusion Science)* (Springer, New York, 1985), p. 830
5. E. Weber, *Molecular Inclusion and Molecular Recognition. Clathrates* (Springer, New York, 1987), p. 266
6. J.V. Smith, *Tetrahedral Frameworks of Zeolites, Clathrates and Related Materials* (Springer, New York, 2000), p. 266

7. R. Xu et al., *Chemistry of Zeolites and Related Porous Materials: Synthesis and Structure* (Wiley, Singapore, 2007), p. 679
8. J.W. Steed, J.L. Atwood, *Supramolecular Chemistry* (Wiley, New York, 2009), p. 970
9. C.A. Koh, *Clathrate Hydrates of Natural Gases* (CRC, Taylor & Francis Group, Boca Raton, 2008), p. 758
10. T. Iwamoto, T. Nakano, M. Morita, T. Miyoshi, T. Miyomoto, Y. Sasaki, Inorg. Chim. Acta. **2**, 313 (1963)
11. T.W. Graham Solomons, *Organic Chemistry*, 6th edn. (Wiley, New York, 1996), p. 1012
12. T. Iwamoto, J. Mol. Struct. **75**, 51 (1981)
13. R.C. Hirt, J.P. Howe, J. Chem. Phys. **16**, 480 (1948)
14. K. Nakamoto, *Infrared and Raman Spectra of Inorganic and Coordination Compounds, Part B*, 5th edn. (Wiley, New York, 1963)
15. K.F. Purcell, R.S. Drago, J. Am. Chem. Soc. **88**, 919 (1966)
16. J.M. Serratosa, Am. Mineral. **53**, 1244 (1968)
17. P.J. Thistlethwaite, Aust. J. Chem. **30**(7), 1595 (1977)
18. D.S. Corrigan, P. Gao, L.-W.H. Leung, M.J. Weaver, Langmuir. **2**, 744 (1986)
19. F. Guillaume, J. Yarwood, A.H. Price, Mol. Phys. **62**(6/20), 1307 (1987)
20. D.W. Boo, K. Kim, M.S. Kim, Bull. Korean Chem. Soc. **8**(4), 251 (1987)
21. A.G. Császár, G. Fogorasi, Spectrochim. Acta, Part A: Mol. Biomol. Spectrosc. **45**(8), 845 (1989)
22. Y. Dimitrova, J. Mol. Struct. (Theochem) **391**(3), 241 (1997)
23. P. Raghuvansh (nee Bhriguvansh), S.K. Srivastava, R.K. Singh, B.P. Asthana, W. Kiefer, Phys. Chem.- Chem. Phys. **6**, 531 (2004)
24. D.W. Boo, K. Kim, M.S. Kim, Bull. Korean Chem. Soc. **9**(1), 27 (1988)
25. R.L. McCullough, L.H. Jones, G.A. Crosby, Spectrochim. Acta **16**, 929 (1960)
26. Z. Kartal, A. Ölmez, Z. Naturforsch. **60a**, 537 (2005)
27. L.J. Bellamy, R.F. Branch, J. Chem. Soc. (Resumed) Issue 0, 4491 (1954)
28. M. Davies, *Infrared Spectroscopy and Molecular Structure* (Elsevier, Amsterdam, 1963)
29. Z. Kartal, Ş. Şentürk, Z. Naturforsch. **60a**, 285 (2005)
30. M. Şenyel, C. Parlak, Ö. Alver, Spectrochim. Acta A **70**, 367 (2008)
31. V.T. Yılmaz, A. Karadağ, Thermochim. Acta **348**, 121 (2000)
32. S. Nishikiori, A. Takahashi, C.I. Ratcliffe, J.A. Ripmeester, J. Supramol. Chem. **2301**, 483 (2002)
33. A. Sopkova, J. Bubanec, J. Therm. Anal. **12**, 97 (1977)
34. C. Parlak, Ö. Alver, M. Şenyel, J. Mol. Struct. **919**, 41 (2009)
35. Z. Kartal, J. Mol. Struct. **938**, 70 (2009)